Improved slow magnetic relaxation in optically pure helicene-based Dy(III) single molecule magnets

Jiang-Kun Ou-Yang, Nidal Saleh, Guglielmo Fernandez-Garcia, Lucie Norel, Fabrice Pointillart, Thierry Guizouarn, Olivier Cador, Federico Totti, Lahcene Ouahab, Jeanne Crassous, et al.

Improved Slow Magnetic Relaxation in Optically Pure Helicene-Based Dy[III] Single Molecule Magnet

J.-K. Ou-Yang,[a] N. Saleh,[a] G. Fernandez Garcia,[a,b] L. Norel,[a] F. Pointillart,[*a] T. Guizouarn,[a] O. Cador,[a] F. Totti,[b] L. Ouahab,[a] J. Crassous,[*a] and B. Le Guennic[*a]

The racemic and optically pure [Dy(hfac)₃(L)] complexes with L = 3-(2-pyridyl)-4-aza[6]-helicene have been synthesized and characterized. Both racemic and enantiopure forms behave as single molecule magnets in their crystalline phase, while electronic circular dichroism activity is evidenced. Ab initio calculations on isolated complexes followed by the determination of intermolecular dipolar couplings allowed the rationalization of the different low-temperature magnetic behaviours. The enantiopure SMM differs from the racemic one by the presence of a hysteresis loop in the former system.

Single Molecule Magnets (SMMs) have drawn the attention of both chemists and physicists communities for more than twenty years because of their potential applications in high-density data storage, quantum computing and spintronics.[1] In molecular magnetism, recent advances consist in combining within a same material several electronic properties that may either simply coexist or strongly interact. Among the potential additional properties, ferroelectricity,[2] conductivity,[3] luminescence,[4] optical activity,[5] non-linear optics[6] have been already explored. A breakthrough came from the synergy between chirality and molecular magnetism with the evidence of strong magneto-chiral dichroism in enantiopure 3D-ordered ferromagnets,[7] and in Single Chain Magnets.[8] Recently, chirality and SMM properties have been merged in the same molecule.[2a,9] In all examples reported so far, differences between the SMM behaviour of the enantiomerically pure and racemic forms have not been evidenced. However, one may expect the possibility to observe different solid-state physical properties for pure enantiomers versus their racemic mixture.[10]
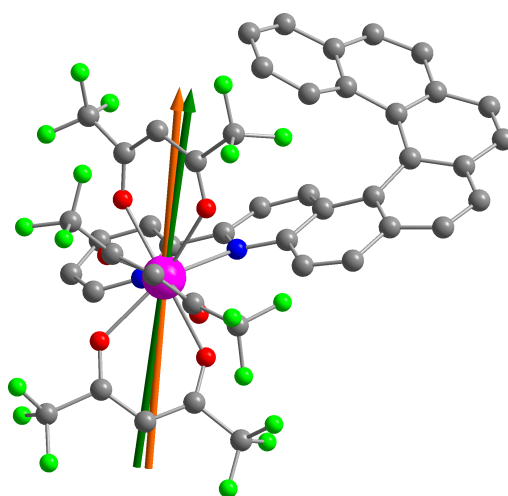

Fig. 1 Representation of the crystallographic structure of **1** in *rac*-**1**·0.5C₆H₁₄. Experimental (dark green) and theoretical (orange) main anisotropy axes. Dy, O, N, C and F are in purple, red, blue, grey and green, respectively. Only the *P* enantiomer is shown and H atoms are omitted for clarity.

On the one hand, [n]helicenes have a π-conjugated helical backbone formed of *ortho*-fused aromatic rings that become configurationally stable when n ≥ 5. As a result of their topology, they display high optical activity and intense emission properties.[11] On the other hand, 2,2'-bipyridine (bpy) derivatives are extensively used as bidentate ligand in coordination chemistry. Thus several Dy[III] coordination complexes involving bpy moiety displayed a SMM behaviour due to the well-adapted electronic distribution given by the N₂O₆ coordination sphere.[12] Consequently, the decoration of a configurationally stable helicene with a bpy fragment appears as an ideal compromise for the coordination reaction to lanthanides, and promising for optimized magnetic and optical properties.

In this communication, we describe the synthesis of mononuclear complexes involving Dy[III] ion and 3-(2-pyridyl)-4-aza[6]-helicene[13] (**L**) in its racemic and optically pure forms. We evidence the strong differences in the static and dynamic magnetic properties of the racemic complex [Dy(hfac)₃(**L**)]·0.5C₆H₁₄ (*rac*-**1**·0.5C₆H₁₄) compared to the pure

a. Institut des Sciences Chimiques de Rennes, UMR 6226 CNRS - Université de Rennes 1, 263 Avenue du Général Leclerc 35042 Rennes Cedex (France).
  E-mail: *fabrice.pointillart@univ-rennes1.fr*, *jeanne.crassous@univ-rennes1.fr*, *boris.leguennic@univ-rennes1.fr*
b. Department of Chemistry "Ugo Schiff" and INSTM RU, University of Florence, 50019 Sesto Fiorentino (Italy).

enantiomers [Dy(hfac)$_3$(**L(-)**)] (**1(-)**) and [Dy(hfac)$_3$(**L(+)**)] (**1(+)**). Finally, ab initio calculations allow the rationalization of the interplay between the solid-state arrangement and the low-temperature behaviours.
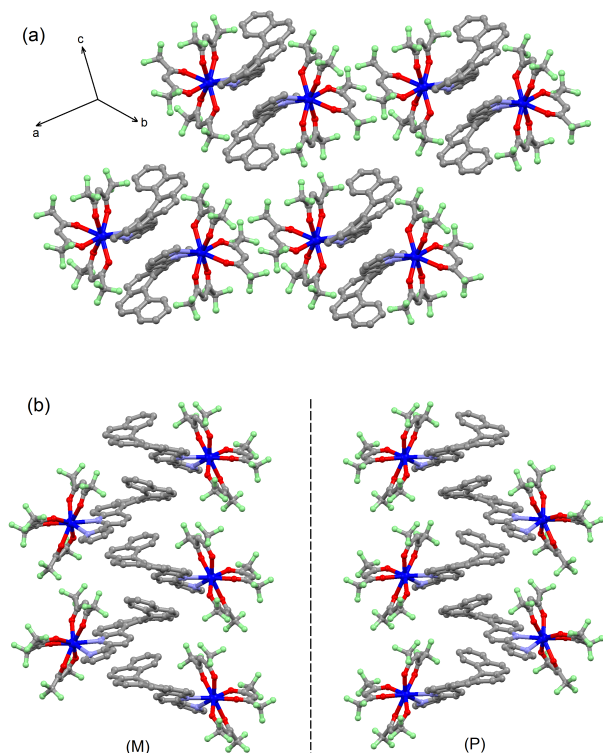

Fig. 2 Crystal packings of (a) *rac*-**1**, (b) **1(-)** (left) and **1(+)** (right) highlighting the (*M*) and (*P*) helicoidal arrangements. The dash line represents the mirror between both enantiomers.

Complex *rac*-**1** was prepared in good yield by reacting racemic mixture of ligand **L** and tris(1,1,1,5,5,5-hexafluoroacetylacetonate)bis(aqueous)Dy^{III} in CH$_2$Cl$_2$. Slow diffusion of *n*-hexane in the mother solution affords yellow single crystals. *rac*-**1** crystallizes in the triclinic centrosymmetric space group P-1 (Fig. 1 and S1, Table S1). The unique Dy^{III} ion resides in a N$_2$O$_6$ triangular dodecahedron environment (D$_{2d}$ symmetry, for SHAPE[14] analysis see SI, Table S2). The six oxygen and two nitrogen atoms come from the three hfac$^-$ anions and one **L** ligand, respectively. Starting from the racemic mixture of **L**, both enantiomers are present in the cell. The crystal packing reveals that heterochiral dimers are formed with the presence of π-π interactions (Fig. 2a). The Dy-Dy shortest intermolecular distance was measured equal to 8.789 Å. Starting from the pure enantiomers **L(-)** and **L(+)**, the complexes **1(-)** (Fig. S2) and **1(+)** (Fig. S3) are obtained (Fig. S4). Both enantiomers crystallize in the non-centrosymmetric P2$_1$2$_1$2$_1$ orthorhombic space group (Table S1). From a molecular point of view, the structures of **1(-)** and **1(+)** are similar to the one of **1** with a Dy^{III} ion in a N$_2$O$_6$ triangular dodecahedron environment (Table S2). Nevertheless, crystal packings highlight drastic changes (Fig. 2b). The **L(-)** or **L(+)** ligands continuously interact through π-π stacking to form (*M*) or (*P*) helical arrangements. The Dy-Dy shortest intermolecular distance is here equal to 10.127 Å that is notably longer than

the distance measured for the racemic mixture. It is worth to mention that the Dy^{III} ion is not a stereogenic centre, but is placed in a chiral environment thanks to the presence of the helicene moiety.

The mirror-image electronic dichroism spectra confirm the configurational stability in solution with Cotton effect of opposite signs at λ$_{max}$ = 370, 354, 334, 275, 266 and 247 nm for each enantiomer (Fig. S5). The ECD spectra of the complexes are very similar to those of the free ligands. No Cotton effect could be attributed to the hfac$^-$ anions and the main part of the optical activity arises from the helicene-based ligand. The specific rotations for **1(-)** ([α]$_D$ = -1050° cm^2 dmol^{-1}) and **1(+)** ([α]$_D$ = +1190° cm^2 dmol^{-1}) are opposite and lower than for **L(-)** and **L(+)** ([α]$_D$ = ±1800° cm^2 dmol^{-1}).
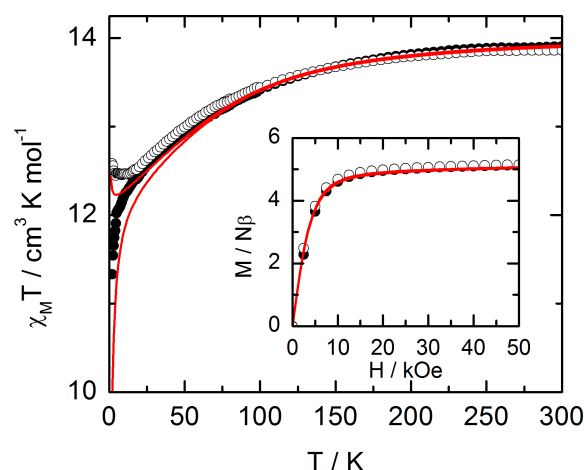

Fig. 3 Temperatures dependences of χ$_M$T for compounds *rac*-**1**·0.5C$_6$H$_{14}$ (black circles) and **1(+)** (white circles). In inset the field variations of the magnetization at 2 K. Full red lines correspond to the simulated curves from *ab-initio* calculations.

As long as high temperatures are concerned no major differences between the magnetic properties of the racemic and enantiomerically pure materials are observed (Fig. 3). Down to 15 K, χ$_M$T's decrease monotonically from 13.95 cm^3 K mol^{-1} (14.17 expected for an isolated Dy^{III} ^{6}H$_{15/2}$ ground state).[15] Only in the low temperature range differences emerge. Indeed, while χ$_M$T decreases continuously on cooling for *rac*-**1**·0.5C$_6$H$_{14}$, in agreement with the depopulation of crystal field sublevels, it slightly increases for **1(+)** and *a fortiori* for **1(-)** (Fig. 3 and S6), thus highlighting possible anti-ferromagnetic couplings in *rac*-**1**·0.5C$_6$H$_{14}$ whereas ferromagnetic interactions are expected for **1(+)** and **1(-)**. The saturation magnetization (~5 Nβ for all compounds) at 2 K confirms that the ground state is essentially described by the Ising components M_J = ±15/2. No evident pathway to promote superexchange interactions between lanthanides emerges from the crystal structures so only dipolar coupling can be supposed to operate here. To shed more light on the already reported results, rotating single-crystal magnetometry in synergy with quantum chemical calculations (CASSCF/SI-SO, see ESI) have been performed on *rac*-**1**·0.5C$_6$H$_{14}$. The orientation of the *g*-tensor, considering the P-1 space group and an effective spin of S = ½, can be routinely determined in measuring the magnetization of a single crystal in three

perpendicular planes (Fig. S7 and S8).[16] As expected, an Ising type anisotropy with the largest g value equal to 18.9 (20 expected for a pure M_J = ±15/2 ground state) was revealed with the orientation of the main magnetic axis along the most negatively charged direction of the coordination polyhedron (Fig. 1).[17] The calculated g-tensor agrees in magnitude as well as in orientation with the experimental findings (Fig. 1 and Table S3). Indeed, the angle between experimental and calculated g_z's is equal to 3.5° while the magnitude of the calculated g_z is 19.8, confirming the Ising type anisotropy. Moreover, the composition of the wavefunction certifies the M_J = ±15/2 nature of the ground state doublet (Table S3).

For **1(+)** (and **1(-)** by extension), the space group $P2_12_12_1$ results in four orientations of the molecules in the crystal, discarding easy experimental determination of the g-tensor. However, the excellent agreement between experimental and *ab initio* data for *rac*-**1** ensures the reliability of the computational results on **1(+)**. The orientation and amplitudes of *g*-tensor are identical to those of *rac*-**1** as well as the composition of the ground state doublet, i.e. mainly M_J = ±15/2 (Table S4 and Fig. S9). Whereas a good agreement is found between the calculated and experimental field-dependence of the magnetization (Inset Fig. 3), it is slightly less straightforward for the $\chi_M T$ *vs*. *T* curves. Indeed, to account for the different magnetic behaviour shown in the low temperature regime (Fig. S10) by the racemic and optically active compounds, the calculation of an average isotropic dipolar coupling J_{dip} generated by the first neighbouring molecules (see SI for computational approach) becomes mandatory. In this framework, anti- (J_{dip} < 0) and ferromagnetic (J_{dip} > 0) interactions between pair of molecules are computed (Fig. S11 and S12, Table S5) in both compounds, but in the case of *rac*-**1**·0.5C_6H_{14} the average dipolar coupling is antiferromagnetic (J_{dip} = -0.055 cm^{-1}) while it becomes ferromagnetic (J_{dip} = 0.0033 cm^{-1}) for **1(+)**. The magnitudes of the average J_{dip} are small with respect to the single pairwise dipolar couplings in both crystal packings, but the latter cancel each other in the averaging, leading to a weak coupling but of different nature. Accounting for this effect in the calculations, an excellent agreement between *ab initio* results and experimental data (Fig. 3) is achieved.

Dynamic magnetic properties also reveal differences between the racemic and enantiomerically pure materials. *rac*-**1**·0.5C_6H_{14} can be seen as a fast SMM with the characteristic maximum on the curves of the out-of-phase component of the ac susceptibility, χ_M'', *vs*. frequency of the oscillating field lying out of the available time window (Fig. S13) for *rac*-**1**·0.5C_6H_{14} at 2 K. For **1(+)** and *a fortiori* **1(-)** such maximum falls at 57 Hz in zero external dc field (Fig. S13 and S14) at 2 K. The τ vs. T curves (τ being the relaxation time of the magnetic moment extracted from the ac *vs*. frequency curves with an extended Debye model, Fig. S14, Tables S6 and S7) for **1(+)** and **1(-)** are represented on Fig. 4. As expected, they are undistinguishable and the relaxation time saturates at low temperature.
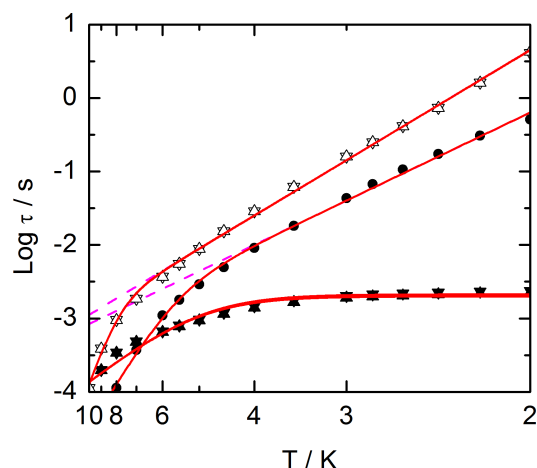
Fig. 4 Log scale plots of the temperature dependence of the relaxation time for **1(+)** and **1(-)** in up and down triangles and *rac*-**1**·0.5C_6H_{14} in circles. Empty symbols indicate measurements in zero external dc field while full symbols indicate measurements at 1 kOe. Red lines correspond to the best-fitted curves with modified Arrhenius laws (see text). Dashed pink lines are the high temperatures extension of the regime reg_1.

This fits with a modified Arrhenius law ($\tau^{-1} = \tau_0^{-1}\exp(-\Delta/kT) + \tau_{TI}^{-1}$) accounting for a temperature independent process provides $\tau_0 \approx 9.5(4)\times10^{-6}$ s, $\Delta \approx 27(3)$ K and $\tau_{TI} = 2.0(2)\times10^{-3}$ s. The application of an external field slows down the relaxation that appears, for **1(+)** (Fig. S15), to be the sum of two relaxation processes: one growing at the expense of the other. The slowest unique relaxation appears at the optimum field of 1 kOe (Fig. S15). For both **1(+)** and **1(-)** the relaxation times follow two thermally activated regimes (reg_0 and reg_1) (Fig. 4 and S16, Tables S8 and S9) with $\tau_0 = 6(6)\times10^{-9}$ s, $\Delta_0 = 101(11)$ K, $\tau_1 = 1.4(2)\times10^{-4}$ s and $\Delta_1 = 21(1)$ K for both **1(+)** and **1(-)**.[18] At 1 kOe the relaxation time of the magnetic moment in *rac*-**1**·0.5C_6H_{14} is tractable (Fig. S17, Table S10) with an extended Debye model. Like for the enantiomerically pure materials two thermally activated regimes (reg_0 and reg_1) are identified with $\tau_0 \approx 9(7)\times10^{-8}$ s, $\Delta_0 \approx 59(5)$ K for the fastest regime reg_0 and $\tau_1 \approx 1.6(3)\times10^{-4}$ s, $\Delta_1 \approx 17(1)$ K for reg_1. Nevertheless, whatever the temperature and the magnetic field, the racemic SMM relaxes much faster than the enantiopure SMM. This is supported by the calculated magnetic transition moments (Fig. S18 and S19) that show a transition probability between the ground-state Kramers doublets which is more than two times higher in the racemic compared to the enantiopure compound.

Hysteresis loops measured at the lowest temperature (500 mK) also suggest different relaxation rates. While the loop is closed at any field for the racemic form it is opened in field for both enantiomerically pure materials (Fig. 5) with a maximum opening of 800 Oe centred at 900 Oe. Of course all the curves shrink at zero field owing to the fast zero field relaxation. At a given field the magnetization of rac-**1**·0.5C_6H_{14} is lower than in **1(+)** and **1(-)** because of the observed antiferromagnetism in the racemic form versus ferromagnetism in the enantiomerically pure material. This example unambiguously illustrates that enantiomerically pure material might show better magnetic properties than the racemic parent depending on the reorganization of the crystal structure between the various forms. As a matter of fact, dissolution of solid materials

in non coordinating solvent such as dichloromethane gives undiscernible magnetic properties for complexes rac-**1** and **1(+)**. The ac susceptibilities at low temperature (2 K) in zero field are identical for rac-**1** and **1(+)** and the in-field behaviours of both χ_M' and χ_M'' are similar (Fig. S20).

In conclusion, we report here a new class of chiral lanthanide-based SMMs, the chirality being induced by the presence of [6]-helicene moieties. These new Dy^{III} SMMs are characterized by notably different magnetic behaviors between the racemic and enantiopure forms. Moreover, such highly configurationally stable chiral molecular magnets can be modified on purpose to be grafted on a surface. This appealing result thus opens new perspectives in both the domains of molecular magnetism and chiral lanthanide complexes since a variety of other systems and properties including circularly polarized luminescence (CPL) activity can be envisioned.
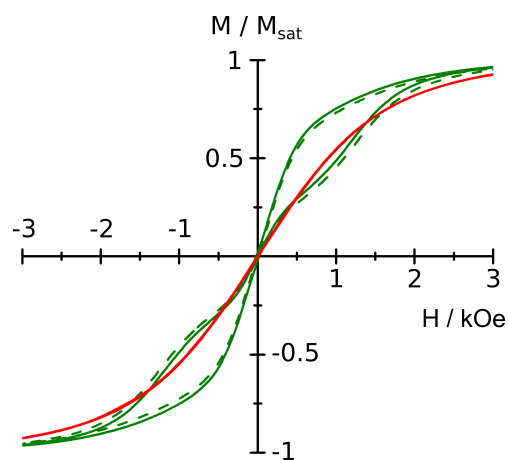

Fig. 5 Magnetic hysteresis loops recorded at 500 mK and measured at a sweep rate of 16 Oe s^{-1} for **1(+)** (full green line), **1(-)** (dashed green line) and *rac*-**1**·0.5C$_6$H$_{14}$ (red line).

Notes and references

1   (a) M. N. Leuenberger, D. Loss, *Nature,* 2001, **410**, 789; (b) M. Mannini, F. Pineider, P. Sainctavit, C. Danieli, E. Otero, C. Sciancalepore, A. M. Talarico, M.-A. Arrio, A. Cornia, D. Gatteschi, R. Sessoli, Nat. Mater., 2009, **8**, 194; (c) S. Thiele, F. Balestro, R. Ballou, S. Klyatskaya, M. Ruben, W. Wernsdorfer, Science, 2014, **344**, 1135; (d) L. Tesi, E. Lucaccini, I. Cimatti, M. Perfetti, M. Mannini, M. Atzori, E. Morra, M. Chiesa, A. Caneschi, L. Sorace, R. Sessoli, Chem. Sci., 2016, **7**, 2074; (e) K. S. Pedersen, A.-M. Ariciu, S. McAdams, H. Weihe, J. Bendix, F. Tuna, S. Piligkos, J. Am. Chem. Soc., 2016, **138**, 5801.

2   (a) J. Long, J. Rouquette, J.-M. Thibaud, R. A. S. Ferreira, L. D. Carlos, B. Donnadieu, V. Vieru, L. F. Chibotaru, L. Konczewicz, J. Haines, Y. Guari, J. Larionova, *Angew. Chem. Int. Ed.*, 2015, **54**, 2236; (b) Y. X. Wang, W. Shi, H. Li, Y. Song, L. Fang, Y. H. Lan, A. K. Powell, W. Wernsdorfer, L. Ungur, L. F. Chibotaru, M. R. Shen, P. Cheng, *Chem. Sci.*, 2012, **3**, 3366.

3   E. Coronado, P. Day, *Chem. Rev.*, 2004, **104**, 5419.

4   (a) K. S. Pedersen, J. Dreiser, H. Weihe, R. Sibille, H. V. Johannesen, M. A. Sørensen, B. E. Nielsen, M. Sigrist, H. Mutka, S. Rols, J. Bendix, S. Piligkos, *Inorg. Chem.*, 2015, **54**, 7600; (b) J. Long, R. Vallat, R. A. S. Ferreira, L. D. Carlos, F. A. Almeida Paz, Y. Guari, J. Larionova, *Chem. Commun.*, 2012, **48**, 9974; (c) F. Pointillart, B. Le Guennic, S. Golhen, O. Cador, O. Maury, L. Ouahab, *Chem. Commun.*, 2013, **49**, 615; (e) F. Pointillart, B. Le Guennic, O. Cador, O. Maury, L. Ouahab, *Acc. Chem. Res.*, 2015, **48**, 2834.

5   S. Chorazy, R. Podgany, W. Nitek, T. Fic, E. Gçrlich, M. Rams, B. Sieklucka, *Chem. Commun.*, 2013, **49**, 6731.

6   C. Train, T. Nuida, R. Gheorghe, M. Gruselle, S.-I. Ohkoshi, *J. Am. Chem. Soc.*, 2009, **131**, 16838.

7   C. Train, R. Ghorghe, V. Krstic, L.-M. Chamoreau, N. S. Ovanesyan, G. L. J. A. Rikken, M. Gruselle, M. Verdaguer, *Nature Mater.*, 2008, **7**, 729.

8   R. Sessoli, M.-E. Boulon, A. Caneschi, M. Mannini, L. Poggini, F. Wilhem, A. Rogalev, *Nature Phys.*, 2015, **11**, 69.

9   (a) R. Inglis, F. White, S. Piligkos, W. Wernsdorfer, E. K. Brechin, G. S. Papaefstathiou, *Chem. Commun.*, 2011, **47**, 3090. (b) C. M. Liu, D.-Q. Zhang, D.-B. Zhu, *Inorg. Chem.*, 2013, **52**, 8933.

10   J. Jacques, A. Collet, S. H. Wilen, *Enantiomers, Racemates, & Resolutions*, J. Wiley & Sons, New York, 1981

11   (a) J. Bosson, J. Gouin, J. Lacour, *Chem. Soc. Rev.*, 2014, **43**, 2824. (b) N. Saleh, C. Shen, J. Crassous, *Chem. Sci.*, 2014, **5**, 3680. (c) C. Shen, E. Anger, M. Srebro, N. Vanthuyne, K. K. Deol, T. D. Jefferson Jr., A. G. Muller, J. A. G. Williams, L. Toupet, C. Roussel, J. Autschbach, R. Réau, J. Crassous, *Chem. Sci.*, 2014, **5**, 1915. (d) K. Nakamura, S. Furumi, M. Takeuchi, T. Shibuya, J. Tanaka, *J. Am. Chem. Soc.*, 2014, **136**, 5555.

12   (a) D.-P. Li, T.-W. Wang, C.-H. Li, D.-S. Liu, Y.-Z. Li, X.-Z.You, *Chem. Commun.*, 2010, **46**, 2929. (b) L. Norel, K. Bernot, M. Feng, T. Roisnel, A. Caneschi, R. Sessoli, S. Rigaut, *Chem. Commun.*, 2012, **48**, 3948. (c) F. Pointillart, J. Jung, R. Berraud-Pache, B. Le Guennic, V. Dorcet, S. Golhen, O. Cador, O. Maury, Y. Guyot, S. Decurtins, S.-X. Liu, L. Ouahab, *Inorg. Chem.*, 2015, **54**, 5384. (d) Y. Bi, Y.-N. Guo, L. Zhao, Y. Guo, S.-Y. Lin, S.-D. Jiang, J. Tang, B.-W. Wang, S. Gao, *Chem. Eur. J.*, 2011, **17**, 12476.

13   (a) N. Saleh, B. Moore, II, M. Srebro, N. Vanthuyne, L. Toupet, J. A. G. Williams, C. Roussel, K. K. Deol, G. Muller, J. Autschbach, J. Crassous, *Chem. Eur. J.*, 2015, **21**, 1673.

14   M. Llunell, D. Casanova, J. Cirera, J. M. Bofill, P. Alemany, S. S. Alvarez, SHAPE (version 2.1), Barcelona, 2013.

15   O. Kahn, *Molecular Magnetism*, VCH: Weinhem, 1993.

16   (a) M.-E. Boulon, G. Cucinotta, J. Luzon, C. Degl'Innocenti, M. Perfetti, K. Bernot, G. Calvez, A. Caneschi, R. Sessoli, *Angew. Chem. Int. Ed.*, 2013, **52**, 350. (b) G. Cucinotta, M. Perfetti, J. Luzon, M. Etienne, P.-E. Car, A. Caneschi, G. Calvez, K. Bernot, R. Sessoli, *Angew. Chem. Int. Ed.*, 2012, **51**, 1606.

17   T. T. da Cunha, J. Jung, M.-E. Boulon, G. Campo, F. Pointillart, C. L. M. Pereira, B. Le Guennic, O. Cador, K. Bernot, F. Pineider, S. Golhen, L. Ouahab, *J. Am. Chem. Soc.*, 2013, **135**, 16332.

18   (a) Y.-N. Guo, G.-F. Xu, P. Gamez, L. Zhao, S.-Y. Lin, R. Deng, J. Tang, H.-J. Zhang, *J. Am. Chem. Soc.*, 2010, **132**, 8538. (b) Y.-N. Guo, L. Ungur, G. E. Granroth, A. K. Powell, C. Wu, S. E. Nagler, J. Tang, L. F. Chibotaru, D. Cui, *Sci. Rep.*, 2014, **4**, 5471.